



Universiteit
Leiden
The Netherlands

PMS2-associated Lynch syndrome : the odd one out

Broeke, S.W. ten

Citation

Broeke, S. W. ten. (2018, September 20). *PMS2-associated Lynch syndrome : the odd one out*. Retrieved from <https://hdl.handle.net/1887/65994>

Version: Not Applicable (or Unknown)

License: [Licence agreement concerning inclusion of doctoral thesis in the Institutional Repository of the University of Leiden](#)

Downloaded from: <https://hdl.handle.net/1887/65994>

Note: To cite this publication please use the final published version (if applicable).

Cover Page



Universiteit Leiden



The handle <http://hdl.handle.net/1887/65994> holds various files of this Leiden University dissertation.

Author: Broeke, S.W. ten

Title: PMS2-associated Lynch syndrome : the odd one out

Issue Date: 2018-09-20

4





**TUMOR
STUDIES**



4.1

Coding microsatellite mutation profiles in cancers of *PMS2* mutation carriers

Manuscript in preparation

Sanne W. ten Broeke*, Alexej Ballhausen*, Aysel Ahadova, Manon Suerink, Hans Morreau, Tom van Wezel, Julia Krzykalla, Axel Benner, Noel de Miranda, Magnus von Knebel Doeberitz, Maartje Nielsen, Matthias Kloor

* These authors contributed equally to this work.

ABSTRACT

Introduction

Lynch syndrome is caused by heterozygous pathogenic germline variants in one of the mismatch repair (MMR) genes (*MLH1*, *MSH2*, *MSH6* and *PMS2*). Lynch syndrome cancers are characterized by MMR deficiency and by the accumulation of multiple insertion/deletion mutations at coding microsatellites (cMS). MMR deficiency-induced mutations at defined cMS loci have a driver function and promote tumorigenesis in Lynch syndrome. However, *PMS2* mutation carriers have only a moderately increased risk of developing colorectal cancer (CRC) or other cancers. In the present study we asked whether the lower penetrance of *PMS2*-associated Lynch syndrome may be reflected by the phenotype of manifest tumors.

Material & Methods

Tumor DNA was extracted from formalin-fixed paraffin-embedded (FFPE) tissue cores (n=90). The mutation spectrum was analyzed by using fluorescently labeled primers specific for a selected series of 18 cMS previously described as mutational targets in MSI cancer development. Immune cell infiltration was analyzed by immunohistochemical staining of FFPE tissue sections for CD3+ T cells.

Results

The cMS spectrum of *PMS2*-associated CRCs did not show any significant differences from other MMR gene-associated CRCs. Most commonly mutant target cMS were located in the genes *ACVR2*, *AIM2*, *BANP*, *C4orf6*, and *ZNF294*. However, *PMS2* tumors displayed a significantly lower CD3+ infiltration ($p=0.0016$).

Discussion

Our observation suggests that MMR deficiency plays a similar role in the pathogenesis of *PMS2*-associated CRCs compared to MMR-deficient cancers lacking functional *MLH1* or *MSH2*. Moreover, our results also imply that the spectrum of cMS mutation-induced frameshift peptide neoantigens of *PMS2*-associated CRCs is expected to be similar to that from other MMR-deficient CRCs. Studies analyzing the mechanisms underlying the lower immune infiltration in *PMS2*-associated cancers are warranted.

INTRODUCTION

Lynch syndrome is caused by a heterozygous pathogenic germline variant in one of the DNA mismatch repair (MMR) genes: *MLH1*, *MSH2* (*EPCAM*), *MSH6* or *PMS2*. After somatic inactivation of the remaining functional MMR gene allele, MMR deficiency leads to the accumulation of numerous small insertions or deletions at repetitive sequence stretches termed microsatellites (microsatellite instability, MSI). Insertions or deletions affecting microsatellites located in gene-encoding regions can lead to shifts of the translational reading frame and thus to inactivation of the affected genes. Moreover, through shifting of the reading frame, completely new peptide stretches are synthesized that are unknown to the immune system and therefore can elicit strong immune responses of the host.^{1,2} Several coding microsatellite mutations that drive Lynch syndrome cancer progression through the inactivation of tumor suppressor genes have been previously identified.^{3,4} As coding microsatellite mutations can contribute to cancer development, the patterns of coding microsatellite mutations observed in manifest cancers reflect evolutionary selection and therefore the pathogenesis of tumor developments. This is for example illustrated by marked differences in coding microsatellite mutation frequency between colorectal and endometrial cancers.^{5,6} *PMS2*-associated Lynch syndrome patients have a markedly lower penetrance and later age of onset of colorectal and endometrial cancer than carriers of *MLH1* or *MSH2* mutations.^{7,8} The reported cumulative risk of CRC is 11-20% for *PMS2* carriers, which is in sharp contrast to a cumulative risk of 35-55% up to age 70 for *MLH1/MSH2* carriers.⁹ Notably, prospective studies have now reported that the cumulative risk of colorectal cancer for *PMS2* mutation carriers undergoing colonoscopic surveillance is 0%.^{10, 11} Again, this is in contrast to *MLH1/MSH2* carriers with risks of CRCs arising between follow-up colonoscopies to be up to 46% and 43% respectively. Even *MSH6* carriers who also have a milder phenotype are at risk (15%) of such interval cancers.¹¹ Consequently, the functional significance of *PMS2* mutations during the pathogenesis of cancers has been questioned and it is perceivable that *PMS2* may play a different and a (minor) role in tumorigenesis. In the present study, we compared coding microsatellite mutation patterns in *PMS2*-associated Lynch syndrome cancers to those observed in colorectal cancers from *MLH1* and *MSH2* mutation carriers.

MATERIAL & METHODS

Tumor specimens

Tumor material from 10 *PMS2* germline mutation carriers was collected within Leiden University Medical Centre (Table 1). Tumor material from 41 *MLH1*, 23 *MSH2*, 12 *MSH6*, and 4 *PMS2* germline mutation carriers was collected within the Department of Applied Tumor Biology, Institute of Pathology, University Hospital Heidelberg, as a center of the German HNPCC Consortium. Informed consent was obtained from all participating patients.

Tumor workup and DNA isolation

Tissue blocks were collected, and DNA was isolated from three tissue cores of variable length (0.3 mm diameter, or 0.7 mm in case of tissue with a low cell count) or from whole tissue sections after manual microdissection using the DNeasy FFPE Kit (Qiagen, Germany).

Microsatellite analysis

For the characterization of cMS patterns, we performed fragment length analysis using fluorescently labeled primers specific for a selected series of 18 coding microsatellites previously described as mutational targets in MSI cancer development.¹² Primer sequences are provided in Table 2. Selection criteria were (1) frequency of mutation in MMR-deficient cancers, (2) evidence of a functional driver role of mutations suggested by a mutation frequency higher than expected from microsatellite length, and (3) potential significance as source of immunogenic frameshift peptide neoantigens supported by epitope prediction algorithms. PCR products were visualized on an ABI3130xl sequencer, and the obtained results were processed using a newly developed algorithm to obtain quantitative estimation of the frequency of the mutant alleles in tumor specimens (qMSI, Ballhausen, Przybilla et al., in preparation).

Immunohistochemical analysis of CD3

From 10 *PMS2*-associated tumors formalin fixed paraffin embedded (FFPE) tumor blocks were available for further analysis of immune cell infiltration. For immunohistochemical detection of CD3⁺ cells, 4 µm thick sections of the tumors were stained with an antibody specific for CD3 (DAKO monoclonal antibody, dilution 1:100). For immune cell scoring 4 areas of interest (0.1 mm² each) were randomly placed in the tumor center, CD3⁺ immune cell infiltration was scored as the mean number of CD3⁺ immune cells of the 4 areas.

TABLE 1 Description of Leiden cohort

Patient ID	Index	Gender	Age at CRC	CRC location	Germline PMS2 mutation	TNM	Differentiation	MSI	IHC	TILs (subjectively scored LUMC)	Mean CD3+ cell count per 0.1mm ²	B2M status
1	Yes	Female	46	Right	c.804-60_804-59in-sJN866832.1	T3N0	Moderate	High	PMS2-/MSH6-	Not scored	N.A.	wildtype
2	Yes	Female	48	Descending colon (flexura lienalis)	c. 856_857delGA (p.Asp286fs)	T3/4N0Mx	Moderate	Not tested	PMS2-/MSH6-	Little	35	wildtype
3	Yes	Male	48	Sigmoid	Deletion exon 5-7	T3N2	Poor	High	PMS2-/MSH6-	Marked	38.25	wildtype
4	No	Female	64	Coecum	c.2192_2196delTAACT (p.Leu731CystsX3)	T4N0	Poor	High	PMS2-/MLH1+	Little	10.75	mutated
5	Yes	Female	46	Rectum (recurrence)	Deletion exon 11-15	T2N0	Moderate	High	PMS2-/MLH1+	Marked	12.5	wildtype
6	Yes	Male	57	Transverse colon	Deletion exon 14	T4N1	Moderate-Poor	High	PMS2-/MLH1+	Little	N.A.	N.A.
7	No	Male	54	Coecum	Deletion exon 5-7	T2N0	Moderate-Poor	High	PMS2-/MLH1+	Moderate	47.75	wildtype
8	Yes	Female	41	Transverse colon	c.736_741delCCCC TinsTGTGTGAAG (p.Pro246CystsX3)	T3N1M1	Poor	Stable	PMS2-/MLH1+	(very) Little	3	wildtype
9	Yes	Male	47	Transverse colon	c.354-1G>A	T2N0	Well-Moderate	High	PMS2-/MLH1+	Moderate	13.75	wildtype
10	Yes	Male	27	Coecum	c.1882C>T (p.Arg628X)	T3N2	Poor	High	PMS2-/MLH1+	Little	27.75	wildtype

CRC: Colorectal cancer

TABLE 2 Primer sequences of the analyzed cMS

Gene name	cMS length	Forward primer	Reverse primer
ACVR2A	A8	GTTGCCATTTGAGGAGGAAA	CAGCATGTTTCTGCCAATAATC
AIM2	A10	TTCTCCATCCAGGTTATTAAGGC	TTAGACCAGTTGGCTTGAATTG
ASTE1	A11	ATATGCCCCCGCTGAAATA	TTGGTGTGTGCAGTGGTTCT
BANP	T12	TTCTGTGGAAGCTCTGCCTT	TCAAGTCGCATCAGATCCAG
C4orf6	T10	CCAGAAGCAAATTCACAAGAC	TTTTGCGTGTTCCCTTCCTTC
CASP5	A10	CAGAGTTATGTCTTAGGTGAAGG	ACCATGAAGAACATCTTTGCCAG
ELAVL3	G9	GATGCGACCTGTTATCTCCAG	AGGTTGGTCTTGCTGTGCTC
GLYR1	G8	GCCTCCAGAAGCTGTGACTT	ATCACCAACATCCCGTCATT
LMAN1	A9	CACCCATGTCAGCTTTGCTA	GGAGGAATTTGAGCACTTCA
MARCKS	A11	GACTTCTTCGCCCAAGGC	GCCGCTCAGCTTGAAAGA
NDUFC2	T9	TGAATTTACAGTTTGCATCG	AACATTTACGGTCCCCTCAC
PTHLH	A11	TTTCACTTTTCAGTACAGCACTTCTG	GAAGTAACAGGGGACTCTTAAATAATG
SLC22A9	A11	GCGCCTACAGTGCCTACTCT	GCATGTGGAGCATTTACAC
SLC35F5	T10	TGTGGGGAAACTTACTGCAA	TCAAGTTTCAAACATCATATGCAA
TAF1B	A11	ACCCAAATAAAAGCCCTCAAC	CTACTTAAAATTCCATTCCATGTCC
TCF7L2	A9	GCCTCTATTCACAGATAACTC	GTTACCTTGTATGTAGCGAA
TGFBR2	A10	GCTGCTTCTCCAAAGTGCAT	CAGATCTCAGGTCCCACACC
ZNF294	A11	AAGCCGAAGAGCTCATTGAA	CAGTTGTTAATTTCCAGCCTTC

Statistical analysis

Statistical significance of differences in mutation rates between tumors from *PMS2* mutation carriers and those from *MLH1* and/or *MSH2* mutation carriers was calculated in three steps.

First, all cMS showing a prevalence of at least 15% non-wild type alleles in a certain tumor were classified as mutant. The distribution of mutation rates was compared between tumors from *PMS2* mutation carriers and those from *MLH1* and *MSH2* mutation carriers grouped together using general mutation frequency of cMS in a chi-squared test. Benjamini-Hochberg procedure was used to adjust the raw p-values over all genes. P values smaller than 0.05 were classified as statistically significant.

In a second step, quantitatively analyzed mutant allele ratios were used to test for differences in cMS mutation patterns between tumors from *PMS2* mutation carriers and those from *MLH1* and *MSH2* mutation carriers grouped together. For this, Wilcoxon-

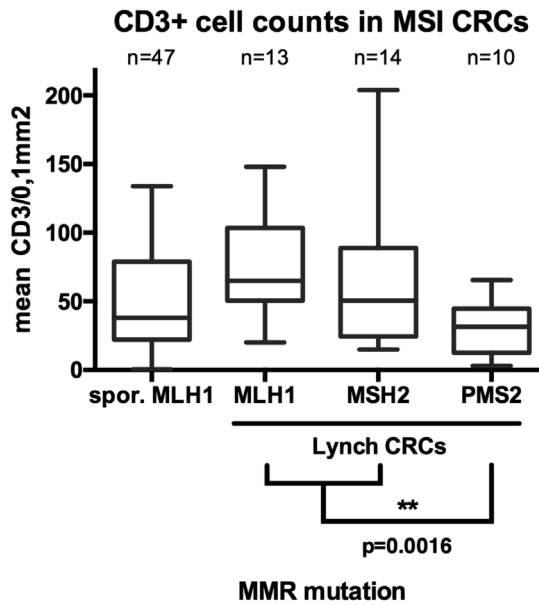


FIGURE 1 Proportion of samples with common hotspot variants G12D and G13D, or other KRAS variants.

Note: p-values represent comparison between PMS2-associated colorectal tumors and MLH1- or MSH2-associated tumors, respectively.

Mann-Whitney test was used and raw p-values were adjusted over all genes using Benjamini-Hochberg procedure.

Finally, quantitatively analyzed cMS patterns of *PMS2* mutation carriers were separately tested against those from *MLH1* and *MSH2* mutation carriers. The global p-value states if there is a significant difference for at least one of the two pairwise comparisons using Wilcoxon-Mann-Whitney test (*PMS2* vs. *MLH1* or *PMS2* vs. *MSH2*). The pairwise p-values give the results for local pairwise comparison. Then, a two-sample Kolmogorov-Smirnov test was applied for the pairwise comparisons in order to test for equal distribution. Pairwise p-values for both approaches were adjusted over all genes using Benjamini-Hochberg procedure. No separate comparison of mutation patterns between tumors from *PMS2* mutation carriers and *MSH6* mutation carriers was performed due to the limited number of *MSH6* mutation carriers available.

Additionally, T-cell infiltration measured by mean number of CD3+ T cells was compared between *PMS2* mutation carriers and *MLH1* and *MSH2* mutation carriers grouped together. Wilcoxon-Mann-Whitney test was applied in order to test the difference in median CD3+ T-cell infiltration between the two groups.

RESULTS

Comparison of cMS mutation frequency between *PMS2* CRCs and non-*PMS2* CRCs

Tumors from 14 *PMS2*, 41 *MLH1*, 23 *MSH2* and 12 *MSH6* mutation carriers were analyzed for cMS mutation patterns. Five out of 18 analyzed cMS showed mutations in all analyzable *PMS2*-associated CRCs: *ACVR2* (n=12), *AIM2* (n=12), *BANP* (n=12), *C4orf6* (n=10), *ZNF294* (n=12). Common functionally relevant target cMS presented with similar mutation frequencies in *PMS2* vs. non-*PMS2*-associated CRCs, including *ACVR2* (*PMS2*: 12/12, 100% vs non-*PMS2*: 46/51, 90.2%, $p=0.59$) and *AIM2* (*PMS2*: 12/12, 100% vs. non-*PMS2*: 42/48, 87.5%). *TGFBR2*, the most commonly analyzed cMS target in MMR-deficient colorectal cancer, displayed a similar frequency of mutations in the *PMS2* vs. the non-*PMS2* CRC collection (*PMS2*: 9/11, 81.8% vs. non-*PMS2*: 41/44, 93.2%, Table 3).

No significant differences in coding microsatellite mutation frequencies were observed between colorectal cancers from *PMS2* mutation carriers and colorectal cancers from *MLH1* and *MSH2* mutation carriers after adjusting for multiple testing (Table 3).

Quantitative analysis of mutant cMS alleles

The time point of MMR deficiency during CRC pathogenesis has previously shown to be related to mutational signatures.¹³ In order to evaluate whether *PMS2*-mutant tumors may show a quantitative difference of cMS mutations compared to *MLH1*- and *MSH2*-deficient CRCs, we quantitatively analyzed mutant allele ratio. The analysis did not reveal any significant difference. However, a trend towards a higher proportion of mutant alleles was observed for the cMS of *C4orf6* (*PMS2*: 0.434, n=10 vs. 0.253, n=47, raw $p=0.004$, Benjamini-Hochberg corrected $p=0.07$). For this candidate, a separate comparison of *PMS2*-associated CRCs with *MLH1*-associated and with *MSH2*-associated CRCs revealed a significant difference between mutation rates of *C4orf6* between the *PMS2* and *MSH2* group (*PMS2*: 0.434; *MSH2*: 0.196, adjusted pairwise $p=0.01$).

TABLE 3 Percentage of tumors harboring mutations

cMS	Mutation frequency (PMS2)	Sample number (PMS2)	Mutation frequency (MLH1+MSH2)	Sample number (MLH1+MSH2)	p value	Adjusted p value
ACVR2A	100,0%	12	90,2%	51	0,5913	1
AIM2	100,0%	12	87,5%	48	0,4514	1
ASTE1	75,0%	12	89,4%	47	0,4096	1
BANP	100,0%	12	95,3%	43	1	1
C4orf6	100,0%	10	59,6%	47	0,0363	0,4198
CASP5	54,5%	11	75,0%	44	0,3346	1
ELAVL3	50,0%	10	64,4%	45	0,6237	1
GLYR1	54,5%	11	58,0%	50	1	1
LMAN1	45,5%	11	54,0%	50	0,8569	1
MARCKS	90,9%	11	88,1%	42	1	1
NDUFC2	76,9%	13	88,6%	44	0,5393	1
PTHLH	66,7%	12	68,0%	50	1	1
SLC22A9	91,7%	12	86,4%	44	1	1
SLC35F5	91,7%	12	55,3%	47	0,0466	0,4198
TAF1B	90,9%	11	82,4%	51	0,8043	1
TCF7L2	75,0%	8	69,8%	43	1	1
TGFBR2	81,8%	11	93,2%	44	0,5577	1
ZNF294	100,0%	12	94,3%	53	0,9346	1

4

Quantitative analysis of intratumoral CD3+ lymphocyte infiltration

As a next step, we analyzed the density of tumor-infiltrating lymphocytes in tumors from *PMS2*, *MLH1* and *MSH2* mutation carriers. The analysis of CD3+ lymphocyte infiltration revealed a significantly lower CD3+ T-cell counts in *PMS2*-associated CRCs when compared to tumors of *MLH1* and *MSH2* mutation carriers (Mann-Whitney test, $p=0.0016$, Figure 1). Interestingly, median CD3+ T-cell counts of *PMS2* mutation carriers were closer to those from sporadic MSI CRCs (38 compared to 31.50, Table 4).

TABLE 4 Frequency of mutant alleles

cMS	Mutant allele ratio (PMS2)	Sample number (PMS2)	Mutant allele ratio (MLH1+MSH2)	Sample number (MLH1+MSH2)	p value	Adjusted p value
ACVR2A	0.503	12	0.506	51	0.6193	0.7962
AIM2	0.523	12	0.426	48	0.0460	0.1901
ASTE1	0.325	12	0.473	47	0.0402	0.1901
BANP	0.483	12	0.570	43	0.2286	0.6179
C4orf6	0.434	10	0.253	47	0.0039	0.0702
CASP5	0.238	11	0.299	44	0.3433	0.6179
ELAVL3	0.191	10	0.246	45	0.3138	0.6179
GLYR1	0.177	11	0.268	50	0.3004	0.6179
LMAN1	0.179	11	0.201	50	0.9779	0.9779
MARCKS	0.341	11	0.414	42	0.2820	0.6179
NDUFC2	0.272	13	0.322	44	0.4571	0.6329
PTHLH	0.315	12	0.334	50	0.9613	0.9779
SLC22A9	0.409	12	0.379	44	0.7007	0.8408
SLC35F5	0.341	12	0.230	47	0.0528	0.1901
TAF1B	0.405	11	0.293	51	0.0114	0.1026
TCF7L2	0.381	8	0.318	43	0.4071	0.6329
TGFBR2	0.3944	11	0.466	44	0.5105	0.7068
ZNF294	0.469	12	0.486	53	0.7959	0.8954

DISCUSSION

PMS2 mutation carriers represent a distinct entity among Lynch syndrome patients, denoted mainly by a lower penetrance, making *PMS2* a moderately penetrant gene at most.^{7, 8, 14} However, recent work has suggested that tumors with *PMS2* deficiency may demonstrate a more aggressive phenotype.¹⁵ These observations suggest that there may be fundamental differences in the pathogenesis of *PMS2*-associated CRCs that distinguish them from Lynch syndrome CRCs caused by germline variants affecting other MMR genes such as *MLH1* and *MSH2*.

So far, the somatic cMS mutation landscape of *PMS2*-associated CRCs has been unknown. We observed very similar somatic mutation patterns in *PMS2*-associated CRCs to those obtained in *MLH1*- and *MSH2*-mutant CRCs. This observation suggests that the role of cMS mutations during the development of *PMS2*-mutant cancers is comparable to cMS mutations in *MLH1*-deficient and *MSH2*-deficient CRCs. This may imply that *PMS2*-mutant colorectal cancers develop through a similar pathogenetic mechanism, with a similar impact of MMR deficiency, compared to other Lynch syndrome-associated cancers. Our results strongly support the hypothesis that MMR deficiency caused by *PMS2* mutations is a significant driving force of tumor development in these cancers rather than representing merely an epiphenomenon.

However, there are reports that *PMS2* deficiency may occur at a relatively late stage of carcinogenesis as illustrated by the reported relatively low frequency of MMR-associated *KRAS* hotspot variants G12D and G13D in a study that included CRCs analyzed here as well.¹⁶ The same study also reported a lack of β -catenin variants in *PMS2*-associated CRCs, while the majority of a *MLH1* control cohort did harbor such variants. β -catenin variants have been suggested to be associated with CRCs that develop from dMMR crypts.^{13, 17} CRCs developing through the dMMR crypt pathway and not through the traditional MMR proficient (pMMR) adenoma to CRC pathway may present as CRCs that develop in between surveillance colonoscopies in Lynch syndrome patients. These tumors may develop more rapidly and perhaps for some part also lack a benign (dMMR) adenoma precursor that can be prevented by a polypectomy.^{13, 17} Indeed, prospective cohorts report low or even absent risk for *PMS2* carriers undergoing regular surveillance and polypectomies if needed (ten Broeke and Suerink et al, 2018, manuscript in preparation).^{10, 11} One of these studies also reported normal *PMS2* expression in 16 adenomas stained with immunohistochemistry, again underlining the possibly late timing of *PMS2* deficiency (ten Broeke and Suerink et al, 2018, in preparation).

In general Lynch-associated CRCs appear to have better prognosis which is believed

to be a consequence of increased immune activation due to frameshift neo-antigens due to cMS.^{1, 18} A recent paper by Alpert and colleagues reported that CRCs with isolated *PMS2* loss due to germline *PMS2* mutations showed trends towards presenting with more distant metastasis and higher disease-specific death when compared to tumors due to pathogenic variants in other MMR genes.¹⁵ They also reported that CRCs with isolated *PMS2* loss have a lower frequency of MSI-related features such as increased tumor-infiltrating lymphocytes (TILs) and Crohn-like infiltrate, suggesting a lower degree of immune activation, possibly explaining their observation of a worse prognosis for *PMS2*-associated CRCs. Our results showing significantly lower CD3+ T-cell counts are in line with this observation and may be a result of later occurrence of *PMS2* deficiency. However, the explanation suggested by Alpert et al. that these tumors may develop less neoantigen-producing mutations could not be confirmed by our study, as no significant differences between *PMS2*-associated CRCs and *MLH1*- or *MSH2*-associated CRCs were detected. However, due to the limited number of analyzed tumor specimens, more subtle differences may have been missed.

Another limitation of our study is that only certain cMS targets selected according to their high likelihood of representing functionally relevant drivers of tumorigenesis were analyzed, so that the level of “irrelevant” background MSI affecting functionally neutral or less significant cMS is not properly reflected by the analysis. Our panel was therefore not properly suited to assess a general estimation of the quantitative level of MSI in *PMS2*-associated tumors. A lower overall amount of MSI could still explain the observation of lower immune response by the host surrounding these tumors. Therefore, further studies on larger sample sets are required to validate our observation of a similar cMS spectrum for all MMR carriers. Due to the similar pattern of neoantigen-inducing cMS, we expect that vaccines developed for the prevention of Lynch syndrome-associated cancers should also cover *PMS2*-mutant tumors. In addition, *PMS2*-mutant CRC patients with metastasized disease may likely benefit from immune checkpoint blockade using anti-PD-1 or anti-PD-L1 antibodies that have shown very promising results in MMR-deficient cancer patients.

In conclusion, while we observed a similar cMS spectrum for *PMS2*-associated CRCs when compared to other Lynch associated tumors we did see lower CD3+ infiltration, possibly suggesting a later occurrence of *PMS2* deficiency. A lower immune response in *PMS2* carriers that develop CRC may have consequences for metastatic potential and overall prognosis, which should be explored in future studies that also include clinical data.

REFERENCES

1. Schwitalle, Y. et al. Immune response against frameshift-induced neopeptides in HNPCC patients and healthy HNPCC mutation carriers. *Gastroenterology* 134, 988-997 (2008).
2. Le, D.T. et al. Mismatch-repair deficiency predicts response of solid tumors to PD-1 blockade. *Science* (2017).
3. Alhopuro, P. et al. Candidate driver genes in microsatellite-unstable colorectal cancer. *Int J Cancer* 130, 1558-1566 (2012).
4. Woerner, S.M. et al. Pathogenesis of DNA repair-deficient cancers: a statistical meta-analysis of putative Real Common Target genes. *Oncogene* 22, 2226-2235 (2003).
5. Kim, T.M., Laird, P.W. & Park, P.J. The landscape of microsatellite instability in colorectal and endometrial cancer genomes. *Cell* 155, 858-868 (2013).
6. Hause, R.J., Pritchard, C.C., Shendure, J. & Salipante, S.J. Classification and characterization of microsatellite instability across 18 cancer types. *Nat Med* 22, 1342-1350 (2016).
7. ten Broeke, S.W. et al. Lynch syndrome caused by germline PMS2 mutations: delineating the cancer risk. *Journal of clinical oncology : official journal of the American Society of Clinical Oncology* 33, 319-325 (2015).
8. Senter, L. et al. The clinical phenotype of Lynch syndrome due to germ-line PMS2 mutations. *Gastroenterology* 135, 419-428 (2008).
9. Barrow, E., Hill, J. & Evans, D.G. Cancer risk in Lynch Syndrome. *Fam.Cancer* 12, 229-240 (2013).
10. Moller, P. et al. Cancer incidence and survival in Lynch syndrome patients receiving colonoscopic and gynaecological surveillance: first report from the prospective Lynch syndrome database. *Gut* (2015).
11. Moller, P. et al. Cancer risk and survival in path_MMR carriers by gene and gender up to 75 years of age: a report from the Prospective Lynch Syndrome Database. *Gut* (2017).
12. Woerner, S.M. et al. SelTarbase, a database of human mononucleotide-microsatellite mutations and their potential impact to tumorigenesis and immunology. *Nucleic Acids Res* 38, D682-689 (2010).
13. Ahadova, A. et al. Three molecular pathways model colorectal carcinogenesis in Lynch syndrome. *Int J Cancer* (2018).

14. Goodenberger, M.L. et al. PMS2 monoallelic mutation carriers: the known unknown. *Genetics in medicine : official journal of the American College of Medical Genetics* 18, 13-19 (2016).
15. Alpert, L. et al. Colorectal Carcinomas With Isolated Loss of PMS2 Staining by Immunohistochemistry. *Arch Pathol Lab Med* (2018).
16. Ten Broeke, S.W. et al. Molecular Background of Colorectal Tumors From Patients With Lynch Syndrome Associated With Germline Variants in PMS2. *Gastroenterology* (2018).
17. Ahadova, A., von Knebel Doeberitz, M., Bläker, H. & Kloor, M. CTNNB1-mutant colorectal carcinomas with immediate invasive growth: a model of interval cancers in Lynch syndrome. *Familial cancer* 15, 579-586 (2016).
18. Kloor, M. & von Knebel Doeberitz, M. The Immune Biology of Microsatellite-Unstable Cancer. *Trends in cancer* 2, 121-133 (2016).